Inflation and rupture of rubber membrane

K. Balakhovsky & K. Y. Volokh

International Journal of Fracture

ISSN 0376-9429
Volume 177
Number 2

Int J Fract (2012) 177:179-190
DOI 10.1007/s10704-012-9764-5

Springer

Int J Fract (2012) 177:179–190
DOI 10.1007/s10704-012-9764-5

ORIGINAL PAPER

Inflation and rupture of rubber membrane

K. Balakhovsky · K. Y. Volokh

Received: 14 February 2012 / Accepted: 16 August 2012 / Published online: 31 August 2012

Abstract Inflation and rupture of a circular rubber membrane is modeled in the present work. It is the first time when a failure description is incorporated in the stress analysis of the rubber membrane. The failure description is enforced by the concept of the *energy limiter* that provides the saturation value for the strain energy indicating the maximal energy which may be dissipated by an infinitesimal material volume. The energy limiter is a material constant that can be calibrated via macroscopic experiments. Particularly, two constitutive theories for Natural and Styrene-Butadiene Rubbers enhanced with the energy limiters calibrated in experiments are used for modeling the membrane inflation and failure. It is found based on the finite element simulations and in a good correspondence with the experimental data that rupture occurs in the center of the membrane when the stretches reach the critical magnitude of ~ 5. It is interesting also that the stresses at the point of rupture are essentially smaller than the rubber strength—the critical stress in the uniaxial tension tests. The latter notion questions the applicability of the concept of the material strength defined in uniaxial tests to the multiaxial strain–stress states.

Keywords Rubber membrane · Inflation · Rupture · Failure · Energy limiters

K. Balakhovsky · K. Y. Volokh (✉)
Faculty of Civil and Environmental Engineering, Technion, Israel Institute of Technology, 32000, Haifa, Israel
e-mail: cvolokh@technion.ac.il

1 Introduction

The modeling of the inflation of rubber membranes is a dearly loved subject: Adkins and Rivlin (1952), Corneliussen and Shield (1961), Foster (1967), Hart-Smith and Crisp (1967), Oden and Sato (1967), Kydoniefs and Spencer (1969), Yang and Feng (1970), Tielking and Feng (1974), Needleman (1977), Fried (1982), Dickey (1983), Kelkar et al. (1985), Grabmuller and Weinitschke (1986), Weinitschke (1987), Chen and Cheng (1996), Li et al. (2001), Verron and Marckmann (2003). The topic culminated in the recent book by Muller and Strehlow (2004), which is completely devoted to rubber balloons.

To the best of the authors' knowledge, however, none of the works considering the membrane deformation addressed also the failure issue. It is perfectly in a row with the traditional approach of solid mechanics to separate stress analysis from failure criteria. Such a separation seems to be unreasonable and the necessity to incorporate a failure description in the constitutive equation is physically appealing and desirable. A simple way to introduce the failure description into constitutive equations was considered by Volokh (2004, 2007, 2008, 2010), where the concept of the energy limiter was introduced. The energy limiter provides the saturation value for the strain energy indicating the maximal energy, which may be dissipated by an infinitesimal material volume. The energy limiter is a material constant that can be calibrated via macroscopic experiments. Alternatively, the failure can be

described by using the continuum-atomistic method as in Dal and Kaliske (2009), for example, or methods of continuum damage mechanics (CMD). CMD methods are also popular for modeling the Mullins effect, which is not considered here: Johnson and Beatty (1995), Huntley et al. (1997), De Tommasi et al. (2008), Elias-Zuniga and Rodriguez (2010), Itskov et al. (2010). Continuum-atomistic and CMD methods are more involved computationally than the methods of energy limiters. Besides, CMD methods are less appealing physically because they include internal variables, which are difficult to interpret and calibrate in experiments.

In the present work we use constitutive theories for Natural and Styrene-Butadiene Rubbers enhanced with the energy limiters calibrated in experiments for modeling the membrane inflation and failure. We find based on the finite element simulations and in a good correspondence with the experimental data that rupture occurs in the center of the membrane when the stretches reach the critical magnitude of ~ 5. It is interesting also that the stresses at the point of rupture are essentially smaller than the rubber strength—the critical stress in the uniaxial tension tests. The latter notion questions the applicability of the concept of the material strength defined in uniaxial tests to the multiaxial strain–stress states.

The paper is organized as follows. The total energy of the axisymmetric membrane is derived in Sect. 2. The constitutive equations of rubber including the failure description are given in Sect. 3. The finite element discretization of the membrane is considered in Sect. 4. The results of the simulation are presented in Sect. 5. A discussion of the results in Sect. 6 completes the work.

2 Total potential energy of axisymmetric membrane

A membrane is in equilibrium when the virtual work of the internal forces, $\delta\Pi_1$, is equal to the virtual work of the external forces, $\delta\Pi_2$, or

$$\delta\Pi = \delta\Pi_1 - \delta\Pi_2 = 0. \tag{2.1}$$

The virtual work of the internal forces can be calculated by varying the total strain energy of the membrane

$$\delta\Pi_1 = \delta \int \psi \, dV, \tag{2.2}$$

where ψ is the strain energy density per unit reference volume V of the membrane.

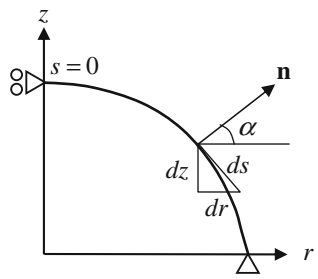

Fig. 1 Axisymmetric membrane

The virtual work of the external forces is the virtual work of pressure, p,

$$\begin{aligned} -\delta\Pi_2 &= -p \int_0^l 2\pi \, r\mathbf{n} \cdot \delta\mathbf{x} \, ds \\ &= 2\pi p \int_0^l r \left(\frac{dz}{ds}\delta r - \frac{dr}{ds}\delta z \right) ds, \end{aligned} \tag{2.3}$$

where

$$\mathbf{n} = \begin{pmatrix} \cos\alpha \\ 0 \\ \sin\alpha \end{pmatrix} = \begin{pmatrix} -dz/ds \\ 0 \\ dr/ds \end{pmatrix}, \quad \delta\mathbf{x} = \begin{pmatrix} \delta r \\ 0 \\ \delta z \end{pmatrix}, \tag{2.4}$$

and s is the arc length of the membrane surface—see Fig. 1.

We notice that it is possible to transform integral (2.3) over the current configuration to the integral over an initial reference configuration introducing the reference arc length, S, such that the current arc length is a unique function of the referential arc length: $s(S)$. After such a substitution we have

$$-\delta\Pi_2 = 2\pi p \int_0^L r \left(z'\delta r - r'\delta z \right) dS, \tag{2.5}$$

where primes designate derivatives with respect to the referential arc length and $l = s(L)$.

It is possible now to introduce the pressure potential explicitly

$$-\Pi_2 = \int_0^L \gamma \left(r, z' \right) dS, \quad \gamma \left(r, z' \right) = p\pi \, r^2 z'. \tag{2.6}$$

Indeed, varying (2.6) we get (2.5)

$$-\delta\Pi_2 = \int_0^L \left(\frac{\partial\gamma}{\partial r}\delta r - \frac{\partial^2\gamma}{\partial S\partial z'}\delta z\right) dS$$

$$= 2\pi p \int_0^L r\left(z'\delta r - r'\delta z\right) dS. \tag{2.7}$$

Thus, equilibrium is provided by the stationary state of the total potential energy

$$\Pi = \Pi_1 - \Pi_2 = \int \psi\, dV + p\pi \int_0^L r^2 z'\, dS. \tag{2.8}$$

In the case of the membrane we can further simplify (2.8) as follows

$$\Pi = \pi \int_0^L \left(2Rh\psi + p\, r^2 z'\right) dS, \tag{2.9}$$

where R is the referential or initial radial coordinate; and h is the initial membrane thickness.

It is worth drawing the reader's attention to the fact that the total potential energy has been written down explicitly given that the pressure potential (2.6) had been found out. The latter result is due to Fried (1982) and it is truly remarkable because generally the hydrostatic pressure load is not conservative. Isaac Fried discovered that in the case of the axisymmetric membrane inflation the pressure load was still displacement-dependent yet conservative.

3 Constitutive equations for rubber

In this section we describe constitutive models of natural (NR) and styrene-butadiene (SBR) rubbers that incorporate a failure description. Energy limiters in the hyperelastic strain energy functions enforce the failure description. The basic physical idea behind the introduction of the energy limiters can be explained as follows. Let us consider an interaction of two particles—Fig. 2.

The interaction undergoes three stages: repulsion, attraction, and separation. The separation starts at the limit point of the force-distance curve shown on the right diagram of Fig. 2. The limit point appears due to the existence of the energy limiter—the bond energy—for the particle potential shown on the left diagram on

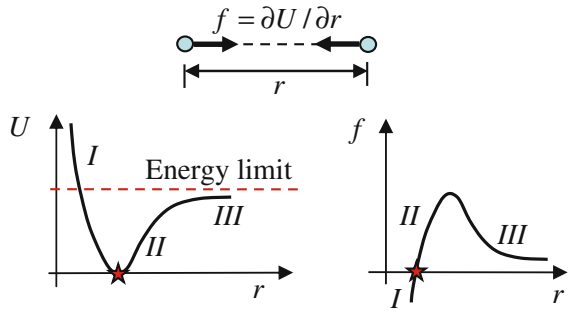

Fig. 2 Particle interaction: *I* repulsion; *II* attraction; *III* separation

Fig. 2. In the case of solids that contain many particles it is impossible to track behavior of individual particles and the concept of continuum is introduced where the averaged characteristics of the particle interaction are described with the help of tensorial measures. For example, the average interparticle distance is measured by a strain tensor and the average particle potential is measured by a strain energy function. However, in contrast to the particle interaction, the classical continuum theories do not include the energy limiters presenting the average bond energy. Thus, the particle separation and, consequently, material failure is beyond the scope of the traditional continuum theories of elasticity: Beatty (1987); Saccomandi and Ogden (2004). However, the failure description can still be introduced in elasticity by analogy with the failure description in the particle interaction: Volokh (2004), Volokh (2007), Volokh (2008), Volokh (2010).

A very simple yet general way to introduce the energy limiters is by using the following formula for the strain energy (Volokh 2007)

$$\psi(\Phi, W) = \Phi\left\{1 - \exp\left(-\frac{W}{\Phi}\right)\right\}, \tag{3.1}$$

where W is the strain energy of an intact, i.e. without failure, material and Φ is the energy limiter, which can also be interpreted as the average bond energy or the failure energy. The energy limiter provides the saturation value for the strain energy indicating the maximum energy that can be stored and dissipated by an infinitesimal material volume.

Formula (3.1) has two limit cases. If the failure energy is infinite, $\Phi \to \infty$, then we have the classical hyperelastic material: $\psi(\infty, W) \to W$. If the failure energy is finite then the increase of the strain energy is limited: $\psi(\Phi, \infty) \to \Phi$.

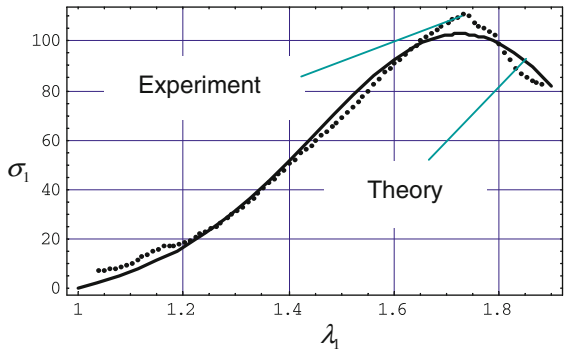

Fig. 3 Cauchy stress [N/cm^2] versus stretch in the uniaxial tension of AAA material (from Volokh and Vorp 2008)

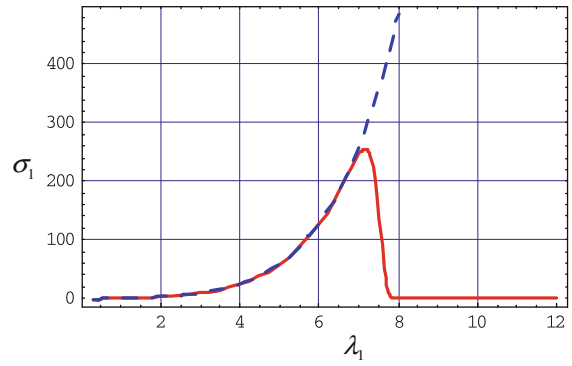

Fig. 4 Cauchy stress [MPa] versus stretch in uniaxial tension of NR: *dashed line* designates the intact model; *solid line* designates the model with energy limiter $\Phi = 82.0$ MPa for $m = 10$

An example of the use of (3.1) can be found in Volokh and Vorp (2008) for the incompressible material of the Abdominal Aortic Aneurysm (AAA) with the intact strain energy in the form $W = \alpha_1(\lambda_1^2 + \lambda_2^2 + \lambda_3^2 - 3) + \alpha_2(\lambda_1^2 + \lambda_2^2 + \lambda_3^2 - 3)^2$, $J = \lambda_1\lambda_2\lambda_3 = 1$, where λ_is are the principal stretches and material constants $\alpha_1 = 10.3$ N/cm^2; $\alpha_2 = 18.0$ N/cm^2; $\Phi = 40.2$ N/cm^2 were calibrated in the uniaxial tension test shown in Fig. 3.

We emphasize that the energy limiter is calibrated in the *macroscopic* failure experiments.

It is evident from Fig. 3 that formula (3.1) is useful for a description of smooth failure with a flat limit point on the stress-strain curve, which corresponds to a gradual process of the bond rupture. In the case of more abrupt bond ruptures, however, a much sharper transition to the material instability occurs. To describe such sharp transition to failure Volokh (2010) modifeied formula (3.1) as follows

$$\psi = \frac{\Phi}{m}\left\{\Gamma\left(\frac{1}{m},\ 0\right) - \Gamma\left(\frac{1}{m},\ \frac{W^m}{\Phi^m}\right)\right\}, \tag{3.2}$$

where the upper incomplete gamma function $\Gamma(s,\ x) = \int_x^\infty t^{s-1}\exp(-t)dt$ is used.

New parameter m controls the sharpness of the transition to material instability on the stress strain curve. Increasing/decreasing m it is possible to simulate more/less steep ruptures of the internal bonds. It should not be missed that (3.2) reduces to (3.1) for $m = 1$.

Formula (3.2) can be applied to a filled NR vulcanizate with the following intact strain energy calibrated by Hamdi et al. (2006)

$$W_{NR} = \sum_{k=1}^{3} C_{k0}(\lambda_1^2 + \lambda_2^2 + \lambda_3^2 - 3)^k,$$
$$J = \lambda_1\lambda_2\lambda_3 = 1, \tag{3.3}$$

where $C_{10} = 0.298$ MPa, $C_{20} = 0.014$ MPa, $C_{30} = 0.00016$ MPa.

Based on the experiments by Hamdi et al. (2006), who found the critical failure stretch in uniaxial tension: $\lambda_c^{NR} = 7.12$, the energy limiter $\Phi = 82.0$ MPa was calibrated for $m = 10$—Fig. 4 (Volokh 2010).

Formula (3.2) can also be applied to a filled SBR vulcanizate with the following intact strain energy calibrated by Hamdi et al. (2006)

$$W_{SBR} = \sum_{k=1}^{2} \frac{\mu_k}{\alpha_k}\left(\lambda_1^{\alpha_k} + \lambda_2^{\alpha_k} + \lambda_3^{\alpha_k} - 3\right),$$
$$J = \lambda_1\lambda_2\lambda_3 = 1, \tag{3.4}$$

where $\mu_1 = 0.638$ MPa, $\alpha_1 = 3.03$, $\mu_2 = -0.025$ MPa, $\alpha_2 = -2.35$.

Based on the experiments by Hamdi et al. (2006), who found the critical failure stretch in uniaxial tension: $\lambda_c^{SBR} = 6.88$, the energy limiter $\Phi = 94.71$MPa was calibrated for $m = 10$—Fig. 5 (Volokh 2010).

At this point we have to emphasize that elasticity with energy limiters does not include a description of the energy dissipation in its theoretical setting. Such description is irrelevant for the static problems considered in the present work because no unloading occurs. However, the account of the dissipation is crucial for modeling dynamic failure where the elastic unloading can potentially lead to the healing of the damaged material. To prevent from the healing, the dissipation should be enforced computationally by removing the failed

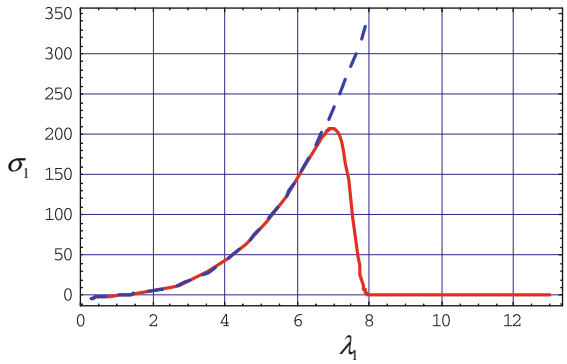

Fig. 5 Cauchy stress [MPa] versus stretch in uniaxial tension of SBR: *dashed line* designates the intact model; *solid line* designates the model with energy limiter $\Phi = 94.71$ MPa for $m = 10$

finite elements from the mesh—see Trapper and Volokh (2010) and Volokh (2011a), for example.

In view of the axisymmetric deformation of the membrane we can describe the deformation gradient in principal stretches

$$\mathbf{F} = \lambda_1 \boldsymbol{\tau} \otimes \boldsymbol{\tau}_0 + \lambda_2 \boldsymbol{\omega} \otimes \boldsymbol{\omega}_0 + \lambda_3 \mathbf{n} \otimes \mathbf{n}_0, \tag{3.5}$$

where

$$\lambda_1 = s' = \sqrt{r'^2 + z'^2}, \quad \lambda_2 = \frac{2\pi r}{2\pi R} = \frac{r}{R},$$
$$\lambda_3 = \frac{1}{\lambda_1 \lambda_2}, \tag{3.6}$$

$$\boldsymbol{\tau} = \begin{pmatrix} \sin\alpha \\ 0 \\ -\cos\alpha \end{pmatrix} = \begin{pmatrix} dr/ds \\ 0 \\ dz/ds \end{pmatrix}, \quad \boldsymbol{\omega} = \mathbf{n} \times \boldsymbol{\tau}$$
$$= \begin{pmatrix} 0 \\ 1 \\ 0 \end{pmatrix}, \quad \mathbf{n} = \begin{pmatrix} \cos\alpha \\ 0 \\ \sin\alpha \end{pmatrix} = \begin{pmatrix} -dz/ds \\ 0 \\ dr/ds \end{pmatrix}, \tag{3.7}$$

$$\boldsymbol{\tau}_0 = \begin{pmatrix} \sin\alpha_0 \\ 0 \\ -\cos\alpha_0 \end{pmatrix} = \begin{pmatrix} dR/dS \\ 0 \\ dZ/dS \end{pmatrix}, \quad \boldsymbol{\omega}_0 = \mathbf{n}_0 \times \boldsymbol{\tau}_0$$
$$= \begin{pmatrix} 0 \\ 1 \\ 0 \end{pmatrix}, \quad \mathbf{n}_0 = \begin{pmatrix} \cos\alpha_0 \\ 0 \\ \sin\alpha_0 \end{pmatrix} = \begin{pmatrix} -dZ/dS \\ 0 \\ dR/dS \end{pmatrix}. \tag{3.8}$$

Equations (3.5)–(3.8) use current quantities r, z, s, $\alpha, \boldsymbol{\tau}, \boldsymbol{\omega}, \mathbf{n}$ and their referential counterparts R, Z, S, $\alpha_0, \boldsymbol{\tau}_0, \boldsymbol{\omega}_0, \mathbf{n}_0$ accordingly.

Based on these kinematic assumptions and the incompressibility condition we have the following constitutive equations for the principal Cauchy stresses

$$\sigma_1 = -g + \lambda_1 \frac{\partial \psi}{\partial \lambda_1}, \quad \sigma_2 = -g + \lambda_2 \frac{\partial \psi}{\partial \lambda_2},$$
$$\sigma_3 = -g + \lambda_3 \frac{\partial \psi}{\partial \lambda_3}, \tag{3.9}$$

where g is indefinite Lagrange multiplier.

Excluding the Lagrange multiplier from (3.9) we get

$$\sigma_1 - \sigma_3 = \lambda_1 \frac{\partial \psi}{\partial \lambda_1} - \lambda_3 \frac{\partial \psi}{\partial \lambda_3}, \quad \sigma_2 - \sigma_3$$
$$= \lambda_2 \frac{\partial \psi}{\partial \lambda_2} - \lambda_3 \frac{\partial \psi}{\partial \lambda_3}, \tag{3.10}$$

The incompressibility condition means that one stretch is not independent $(3.6)_3$ and for a thin membrane we can assume: $\sigma_3 = 0$. In view of these notions we can simplify (3.10) to

$$\sigma_1 = \lambda_1 \frac{\partial \psi}{\partial \lambda_1}, \quad \sigma_2 = \lambda_2 \frac{\partial \psi}{\partial \lambda_2}. \tag{3.11}$$

Remark Calibration of energy limiters and, in a general prospect, strength of materials is based on the assumption that failure occurs homogeneously and material particles break simultaneously. The latter is an idealization that is presented by the limit/peak point on the stress-strain curve. Clearly, real materials are not ideal and they fail inhomogeneously depending on material features and imperfections[1] of a particular specimen. Thus, failure normally localizes into cracks. If so, the question should be asked whether the concept of material strength (or energy limiter) is physically reasonable. The answer can be found in experimental observations on failure of various specimens of the same material under similar loads. If the critical load scatters significantly for various specimens then there is no 'strength of material'. If the critical load does not scatter significantly and cracks appear at approximately the same load then material has strength (and the energy limiter can be calibrated). To the best of the authors' knowledge most specimens fail at approximately the same loads for the same material, thus, supporting the concept of strength. Though, it is generally impossible to exactly predict *where* cracks will appear under the homogeneous deformation it is possible to predict *when* they will appear. Evidently, localization into cracks occurs near the peak/limit point on the stress-strain curve. Does it happen before or after

[1] By imperfections we do not mean macroscopic cracks, notches etc, which trigger the macroscopic stress concentration, rather, we mean imperfections on the size of the internal material structure.

the critical point? In ductile materials, it is believed, the shear bands triggering cracks occur past the critical point on the stress-strain curve. In brittle materials and rubber it is reasonable to assume that material imperfections lead to localization of failure before the ideal critical point is reached. Anyway, localization occurs in the vicinity of the critical point making the concept of strength of materials and energy limiters useful. Needless to say, finally, that structural design is based heavily on the concept of strength of materials and it proved itself superbly.

4 Discretization

In this section we discretize the problem. We partition the membrane into finite elements of equal length l_e and approximate functions within the eth element according to

$$R_e(\xi) = \frac{1}{2}\xi(\xi-1)R_{e1} + (1-\xi^2)R_{e2} + \frac{1}{2}\xi(\xi+1)R_{e3}, \tag{4.1}$$

$$r_e(\xi) = \frac{1}{2}\xi(\xi-1)r_{e1} + (1-\xi^2)r_{e2} + \frac{1}{2}\xi(\xi+1)r_{e3}, \tag{4.2}$$

$$z_e(\xi) = \frac{1}{2}\xi(\xi-1)z_{e1} + (1-\xi^2)z_{e2} + \frac{1}{2}\xi(\xi+1)z_{e3}, \tag{4.3}$$

$$\frac{dr_e(\xi)}{d\xi} = \left(\xi-\frac{1}{2}\right)r_{e1} - 2\xi r_{e2} + \left(\xi+\frac{1}{2}\right)r_{e3}, \tag{4.4}$$

$$\frac{dz_e(\xi)}{d\xi} = \left(\xi-\frac{1}{2}\right)z_{e1} - 2\xi z_{e2} + \left(\xi+\frac{1}{2}\right)z_{e3}, \tag{4.5}$$

where $\xi \in [-1, 1]$ is a local coordinate; and R_{ei}, r_{ei}, z_{ei} are the nodal values of $R_e(\xi)$, $r_e(\xi)$, $z_e(\xi)$ accordingly.

Noticing that

$$dS = l_e d\xi, \quad (\ldots)' = \frac{1}{l_e}\frac{d(\ldots)}{d\xi}, \tag{4.6}$$

we calculate

$$r'_e(\xi) = \frac{1}{l_e}\left\{\left(\xi-\frac{1}{2}\right)r_{e1} - 2\xi r_{e2} + \left(\xi+\frac{1}{2}\right)r_{e3}\right\}, \tag{4.7}$$

$$z'_e(\xi) = \frac{1}{l_e}\left\{\left(\xi-\frac{1}{2}\right)z_{e1} - 2\xi z_{e2} + \left(\xi+\frac{1}{2}\right)z_{e3}\right\}. \tag{4.8}$$

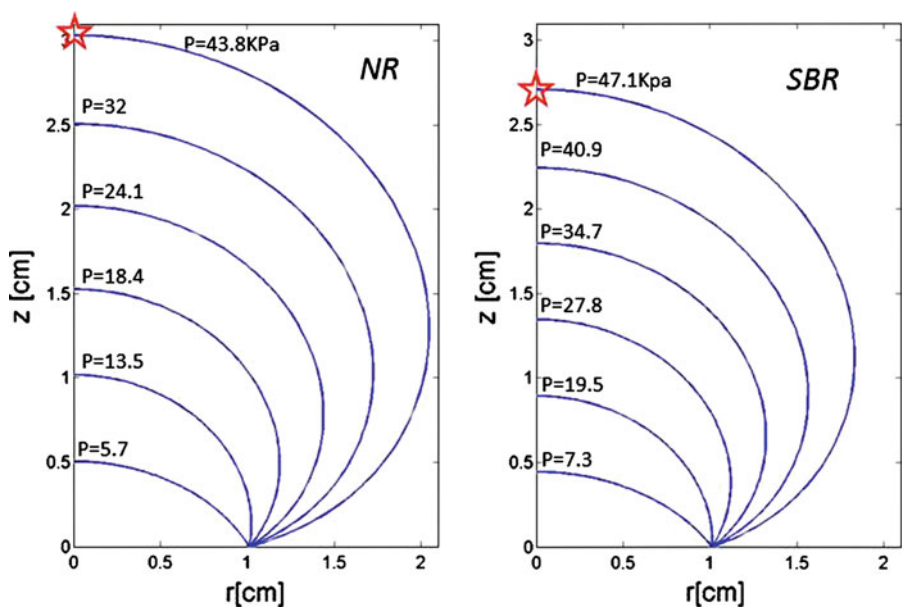

Fig. 6 Inflation of NR and SBR membranes under the increasing hydrostatic pressure; stars designate points of rupture

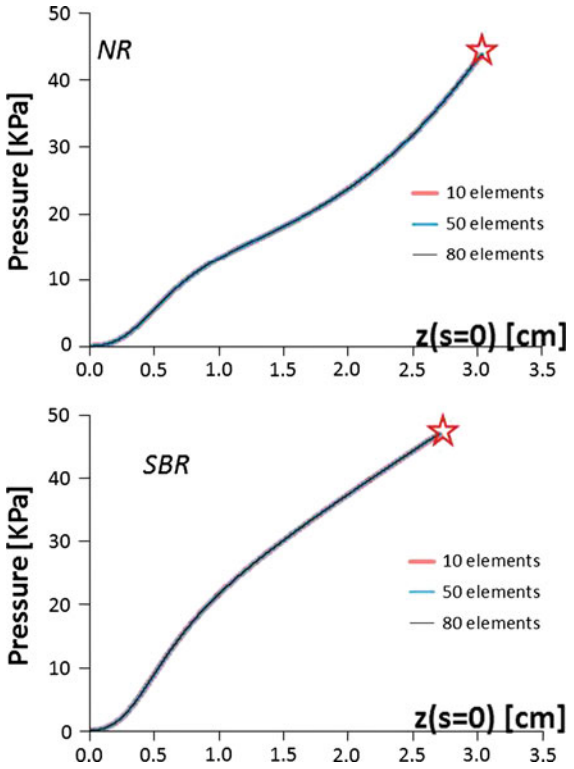

Fig. 7 Pressure versus vertical displacement at the central point for various finite element meshes; *stars* designate points of rupture

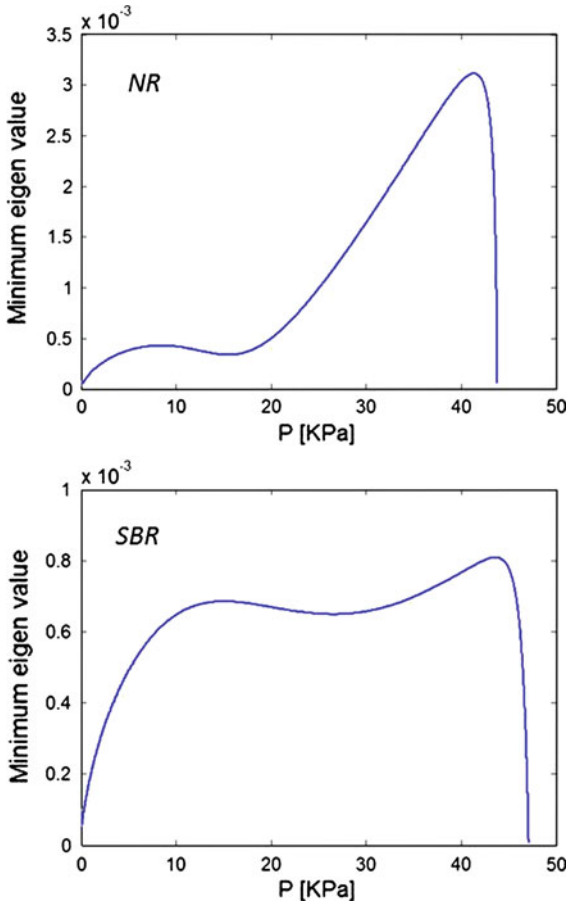

Fig. 8 Minimum eigenvalue of the Hessian of the total energy (tangent stiffness matrix) versus the increasing hydrostatic pressure

The squared stretches of the membrane element (3.6) take form

$$\lambda_{1e}^2(\xi) = r'^2_e(\xi) + z'^2_e(\xi), \quad \lambda_{2e}^2(\xi) = \frac{r_e^2(\xi)}{R_e^2(\xi)},$$
$$\lambda_{3e}^2(\xi) = \frac{1}{\lambda_{1e}^2(\xi)\lambda_{2e}^2(\xi)}. \tag{4.9}$$

Then, the total energy of the element, (2.9), can be written as follows

$$\Pi = \sum_e \Pi_e, \tag{4.10}$$

$$\Pi_e = \pi \int_{-1}^{1} \left(2R_e h_e \psi_e + p\, r_e^2 z'_e\right) l_e \, d\xi. \tag{4.11}$$

Integrating the previous expression at two Gauss points: $\xi_1 = -1/\sqrt{3}$ and $\xi_2 = 1/\sqrt{3}$ we get the spatial approximation

$$\Pi_e \approx \pi\, l_e\{2R_e(\xi_1)h_e\psi_e(\xi_1) + p r_e^2(\xi_1) z'_e\,(\xi_1) + 2R_e(\xi_2)h_e\psi_e(\xi_2) + p r_e^2(\xi_2) z'_e\,(\xi_2)\}. \tag{4.12}$$

5 Results

In the present section we report the results of the numerical simulations of the inflation of a plane circular membrane of radius 1 cm and thickness 0.01 cm fixed at its edge as shown in Fig. 1. The pressure was increased gradually in a quasistatic mode until rupture that occurred in the center of the membrane as shown in Fig. 6. The found critical pressure was $\sim$ 44 KPa for NR and $\sim$ 47 KPa for SBR.

The equilibrium path increased monotonically Fig. 7 and it ended up at the point of rupture where no further equilibrium solution existed. The coincident results were obtained on three finite element meshes for the half-membrane which included 10, 50 and 80 elements.

Since the problem was conservative—see Sect. 2—it was reasonable to track the minimum eigenvalue of

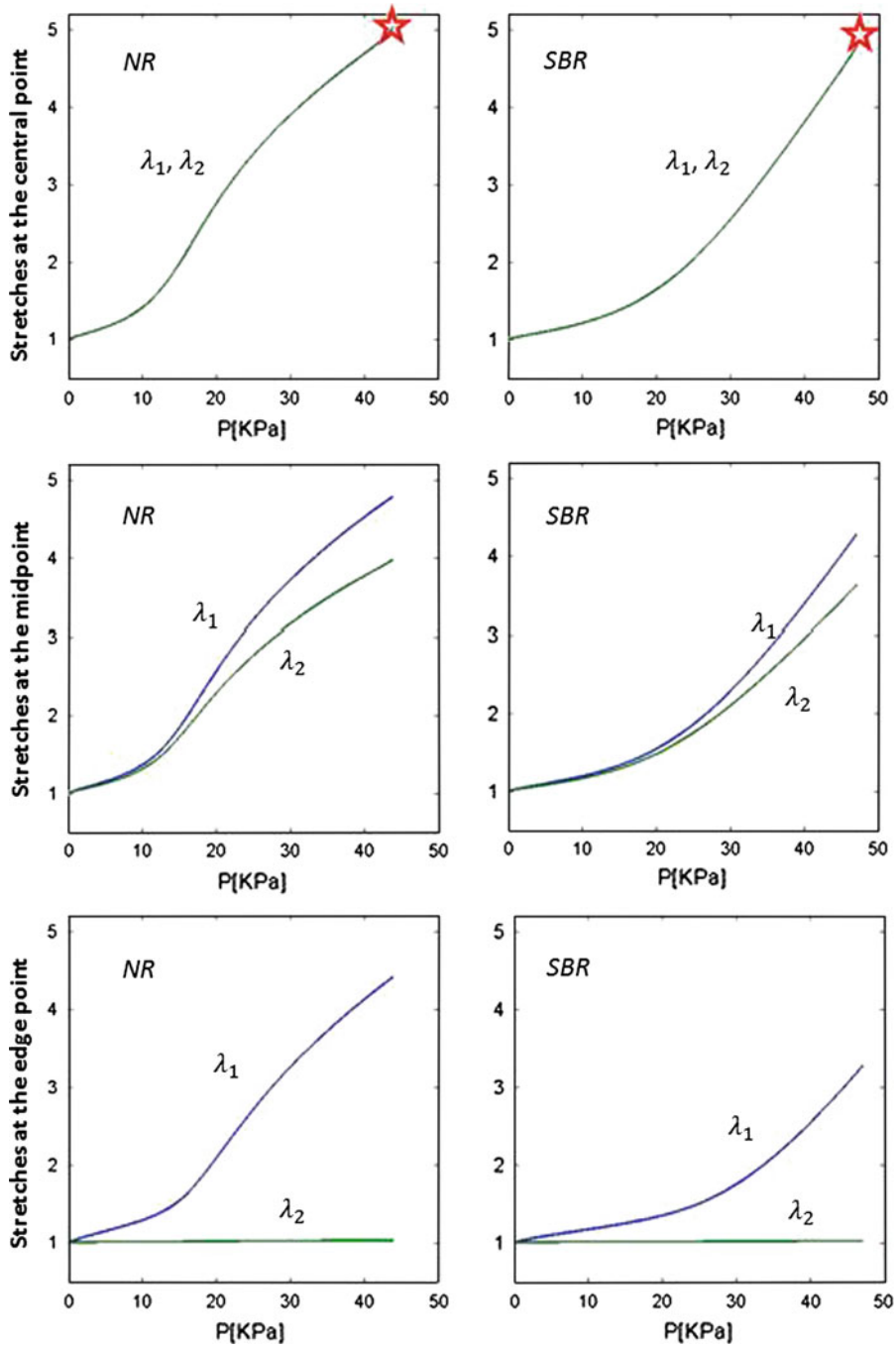

Fig. 9 Principal stretches at the central, mid-, and edge-points of the inflating membrane; *stars* designate points of rupture

the Hessian of the total energy or the tangent stiffness matrix. The varying minimum eigenvalue drops to zero at the point of rupture—Fig. 8.

It was also interesting to track the changing principal stretches and stresses at the center, at the midpoint, and at the edge of the membrane—Figs. 9 and 10. Expectedly, the stretches and stresses dominated at the center of the membrane.

It is remarkable that the critical principal stresses corresponding to the event of rupture were significantly lower in the case of the membrane inflation than in the case of the uniaxial tension shown in Figs. 4 and 5.

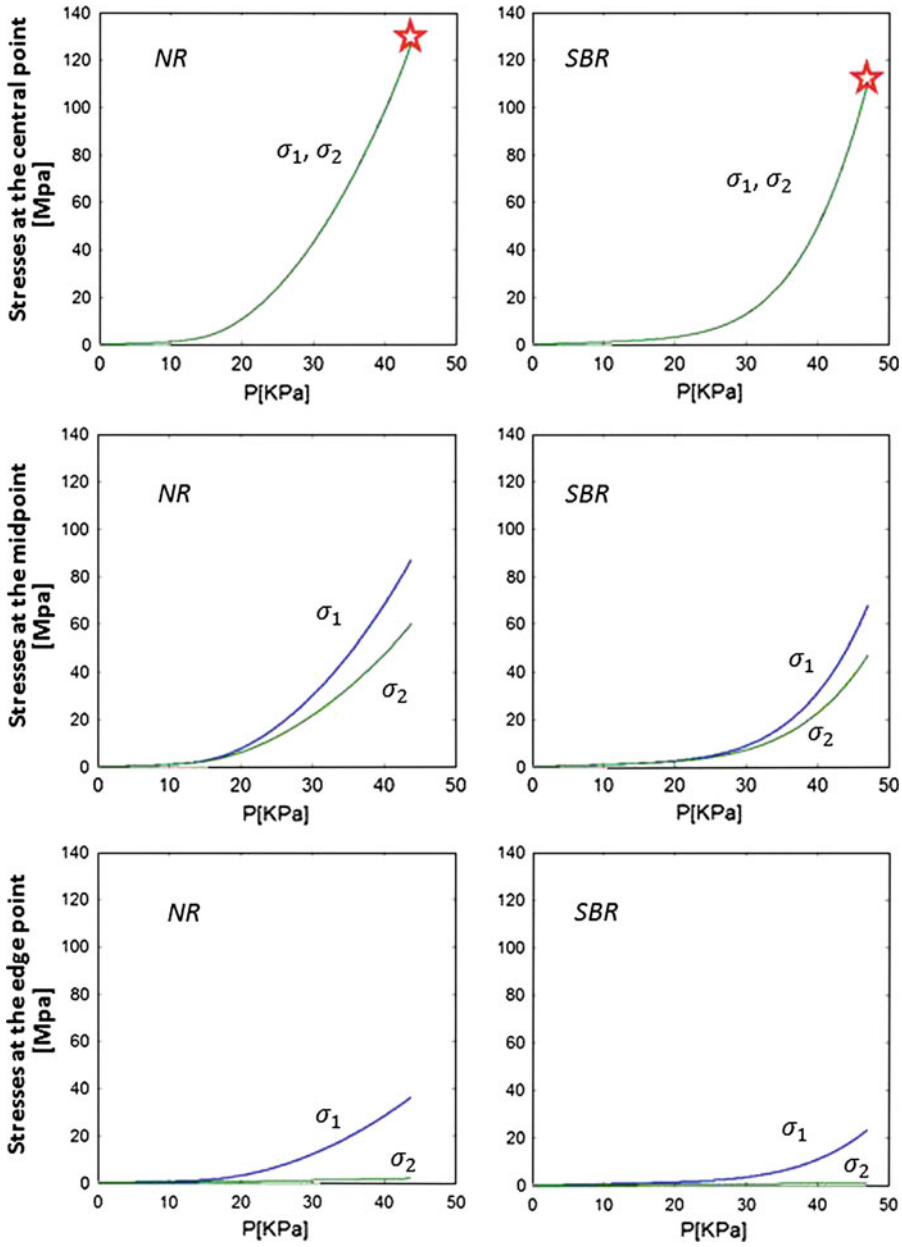

Fig. 10 Principal stresses at the central, mid-, and edge-points of the inflating membrane; *stars* designate points of rupture

Thus, the concept of the material strength defined as the critical stress determined in the uniaxial tension tests is open for criticism.

Finally, the strain energy density is present at the center, at the midpoint, and at the edge of the membrane in Fig. 11.

The reader should not miss that the magnitudes of the strain energy density at the points of rupture cannot exceed the theoretical limits

$$\psi^{\max} = \frac{\Phi}{m}\Gamma\left(\frac{1}{m},\ 0\right) = 78\ [\text{MPa}], \tag{5.1}$$

in the case of NR and

$$\psi^{\max} = \frac{\Phi}{m}\Gamma\left(\frac{1}{m},\ 0\right) = 90\ [\text{MPa}], \tag{5.2}$$

in the case of SBR.

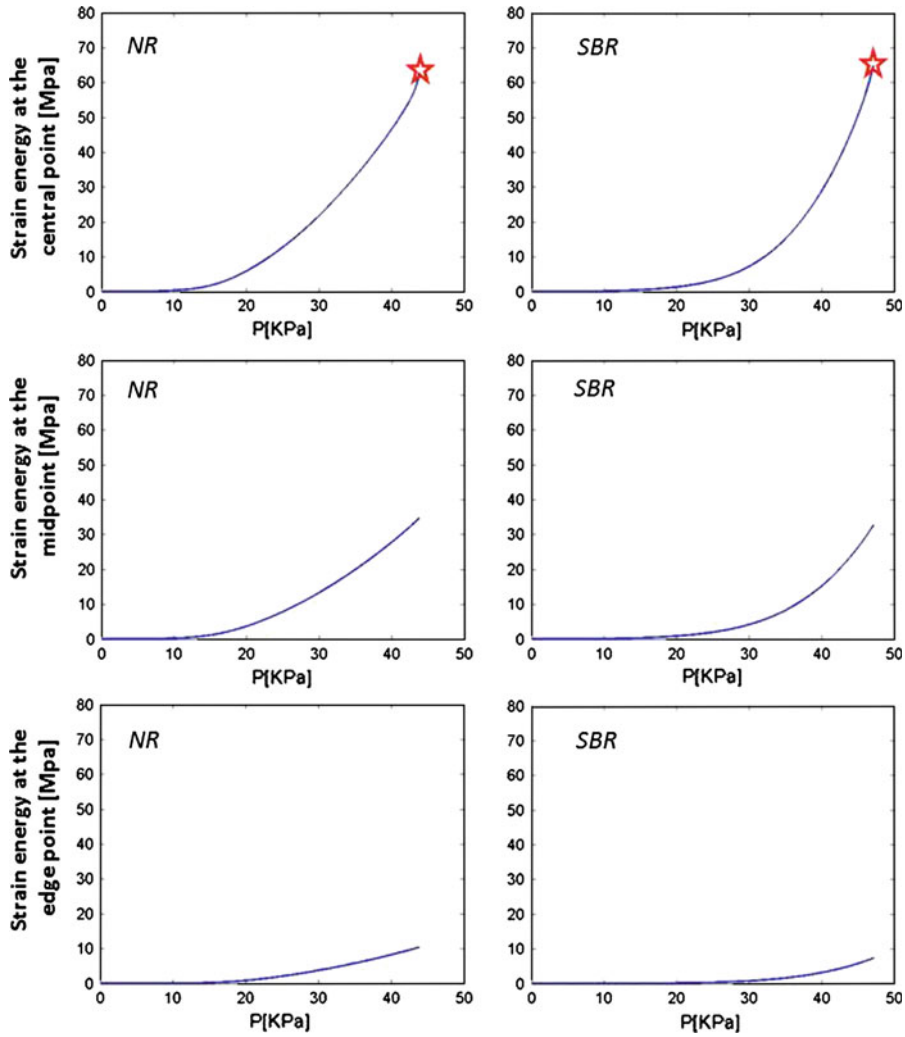

Fig. 11 Strain energy density at the central, mid-, and edge-points of the inflating membrane; *stars* designate points of rupture

6 Discussion

The problem of the inflation of a rubber membrane is one of the oldest in the field of mechanics of rubber-like materials. Ronald Rivlin, largely the founder of the field, addressed this problem in his classical series of papers. Since then the problem is a subject of the constant interest. It is remarkable that all previous studies did not consider failure as a result of inflation while real membranes do fail.

To model failure we limited the capacity of material to accumulate and dissipate the strain energy. The idea of limiting the strain energy density has deep physical roots because it introduces the average energy of molecular/atomic bonds in the continuum description of the bulk. Technically, the idea was implemented by a special choice of the strain energy function, formula (3.2), where a constant, Φ, called the energy limiter was introduced. The energy limiter is a material parameter that is calibrated in macroscopic experiments as any other material parameter. Particularly, to calibrate NR and SBR the uniaxial tension test data had been used including failure. As it was described in Sect. 3, the energy limiter $\Phi = 82.0$ MPa was fitted to the rupture of the NR sample at the critical stretch $\lambda_c^{NR} = 7.12$ and the energy limiter $\Phi = 94.71$ MPa was fitted to the rupture of the SBR sample at the critical stretch $\lambda_c^{SBR} = 6.88$.

The calibrated strain energy function incorporating the energy limiters allowed for a constitutive description of any deformation and not just the one used for calibration. It was important thus to examine the

theory considering various sorts of deformation. The problem of the membrane inflation gave an opportunity to examine the theory in the case of the biaxial deformation. According to the results of the finite element analysis presented in Sect. 5, the failure starts at the center[2] of the inflated membrane where stretches reach the critical magnitude of ~ 5. According to tests of Hamdi et al. (2006), the failure starts at the center of the inflated membrane where stretches reach the critical magnitude of ~ 4.5. The experimentally observed critical stretches are slightly lower than the theoretically predicted ones because of the effects of the material and geometrical imperfections, which escape the idealized theoretical formulation. Nonetheless, the ability of the theory to predict failure seems to be encouraging. It was also found that the stresses at the point of rupture were essentially smaller than the rubber strength—the critical stress in the uniaxial tension tests. The latter finding questions the applicability of the concept of the material strength, defined in uniaxial tests, to the multiaxial strain–stress states.

We must note at this point that we used experimental results of Hamdi et al. (2006) to compare them to the developed theory while another set of very similar experiments was performed by Kawabata (1973) much earlier. The latter author reported critical stretches of approximately ~6.5–7.0 in uniaxial tension for natural rubber close to the results of Hamdi et al. (2006). However, according to Kawabata (1973) these critical stretches practically do not change under the developing biaxiality of the stress-stretch state whereas according to Hamdi et al. (2006) the critical stretches decrease with the developing biaxiality. The experimental data of two groups is controversial and more experiments are required. From the theoretical standpoint results of Kawabata (1973) can be explained by material anisotropy. Indeed, applying the concept of energy limiters to anisotropic materials Volokh (2011b) found that critical stretches might not be affected by the developing biaxiality for some anisotropic rubberlike materials. If material is isotropic then the developing biaxiality should reduce the critical stretch. The latter conclusion also clearly follows from the recent theoretical analysis by Dal and Kaliske (2009) who considered a multiscale structural model of rubber enforced with the rupture of individual bonds. Undoubtedly, more experimental and theoretical studies are necessary to shed more light on the experimental controversy.

Finally, we should note that after the onset of rupture and because of the material and geometrical imperfections in the real membrane the failure should localize into the propagating crack(s). This stage is of great interest too yet it is beyond the scope of the present work.

Acknowledgments This Research Was Supported by General Research Fund at the Technion.

[2] It is interesting to note that inflating aneurysms in the cardiovascular system of the man also tend to rupture at the center similar to the inflating rubber membranes.

References

Adkins JE, Rivlin RS (1952) Large elastic deformations of isotropic materials IX. The deformation of thin shells. Phil Trans R Soc A 244:505–531

Beatty MF (1987) Topics in finite elasticity: hyperelasticity of rubber, elastomers and biological tissues—with examples. Appl Mech Rev 40:1699–1734

Chen D, Cheng S (1996) Non-linear analysis of prestretched circular membrane and a modified iteration technique. Int J Solids Struct 33:545–553

Corneliussen AH, Shield RT (1961) Finite deformation of elastic membranes with application to the stability of an inflated and extended tube. Arch Ration Mech Anal 17:273–304

Dal H, Kaliske M (2009) A micro-continuum-mechanical material model for failure of rubber- like materials: application to ageing-induced fracturing. J Mech Phys Solids 57:1340–1356

De Tommasi D, Puglisi G, Saccomandi G (2008) Localized versus diffuse damage in amorphous materials. Phys Rev Lett 100:1–4

Dickey RW (1983) The nonlinear circular membrane under a vertical force. Quart J Mech Appl Math 41:331–338

Elias-Zuniga A, Rodriguez CA (2010) A non-monotonous damage function to characterize stress-softening effects with permanent set during inflation and deflation of rubber balloons. Int J Engng Sci 48:1937–1943

Foster HO (1967) Very large deformations of axially symmetrical membranes made of Neo-Hookean materials. Int J Eng Sci 5:95–117

Fried I (1982) Finite element computation of large rubber membrane deformations. Int J Num Meth Eng 18:653–660

Grabmuller H, Weinitschke HJ (1986) Finite displacements of annular elastic membranes. J Elasticity 16:135–147

Hamdi A, Nait Abdelaziz M, Ait Hocine N, Heuillet P, Benseddiq N (2006) A fracture criterion of rubber-like materials under plane stress conditions. Polymer Test 25:994–1005

Hart-Smith LJ, Crisp JDC (1967) Large elastic deformations of thin rubber membranes. Int J Eng Sci 5:1–24

Huntley HE, Wineman AS, Rajagopal KR (1997) Stress softening, strain localization and permanent set in the circumfer-

ential shear of an incompressible elastomeric cylinder. IMA J Appl Math 59:309–338

Johnson MA, Beatty MF (1995) The Mullins effect in equibiaxial extension and its influence on the inflation of a balloon. Int J Eng Sci 33:223–245

Itskov M, Ehret AE, Kazakeviciute-Makovska R, Weinhold GW (2010) A thermodynamically consistent phenomenological model of the anisotropic Mullins effect. ZAMM 90:370–386

Kawabata S (1973) Fracture and mechanical behavior of rubberlike polymers under finite deformation in biaxial stress field. J Macromol Sci Phys B 8(3–4):605–630

Kelkar A, Elber W, Raju IS (1985) Large deflections of circular isotropic membranes subjected to arbitrary axisymmetric loading. Comp Struct 21:413–421

Kydoniefs AD, Spencer AJM (1969) Finite axisymmetric deformation of an initially cylindrical elastic membrane. Q J Mech Appl Math 20:88–95

Li Y, Nemes JA, Derdouri AA (2001) Membrane inflation of polymeric materials: Experiments and finite element simulations. Polymer Eng Sci 41:1399–1412

Muller I, Strehlow P (2004) Rubber and rubber balloons: paradigms of thermodynamics. Springer, Berlin

Needleman A (1977) Inflation of spherical rubber balloons. Int J Solids Struct 13:409–421

Oden JT, Sato T (1967) Finite strains and displacements of elastic membranes by the finite element method. Int J Solids Struct 3:471–488

Saccomandi G, Ogden RW (2004) Mechanics and thermomechanics of rubberlike solids. Springer, New York

Tielking JT, Feng WW (1974) The application of the minimum potential energy principle to nonlinear axisymmetrical membrane problems. J Appl Mech 41:491–496

Trapper P, Volokh KY (2010) Modeling dynamic failure in rubber. Int J Fract 162:245–253

Verron E, Marckmann G (2003) Numerical analysis of rubber balloons. Thin-Walled Struct 41:731–746

Volokh KY (2004) Nonlinear elasticity for modeling fracture of isotropic brittle solids. J Appl Mech 71:141–143

Volokh KY (2007) Hyperelasticity with softening for modeling materials failure. J Mech Phys Solids 55:2237–2264

Volokh KY (2008) Multiscale modeling of material failure: from atomic bonds to elasticity with energy limiters. J Multiscale Comput Eng 6:393–410

Volokh KY (2010) On modeling failure of rubber-like materials. Mech Res Com 37:684–689

Volokh KY (2011a) Characteristic length of damage localization in rubber. Int J Fracture 168:113–116

Volokh KY (2011b) Modeling failure of soft anisotropic materials with application to arteries. J Mech Behav Biomed Mater 4:1582–1594

Volokh KY, Vorp DA (2008) A model of growth and rupture of abdominal aortic aneurysm. J Biomech 41:1015–1021

Weinitschke HJ (1987) On finite displacements of circular elastic membranes. Math Meth Appl Sci 9:76–98

Yang WH, Feng WW (1970) On axisymmetrical deformations of nonlinear membranes. J Appl Mech 37:1002–1011